Time-Resolved Fluorescence Study of Aggregation-Induced Emission Enhancement by Restriction of Intramolecular Charge Transfer State

Bing-Rong Gao,[†] Hai-Yu Wang,*,[†] Ya-Wei Hao,[†,‡] Li-Min Fu,[§] Hong-Hua Fang,[†] Ying Jiang,[†] Lei Wang,[†,‡] Qi-Dai Chen,[†] Hong Xia,[†] Ling-Yun Pan,[†,‡] Yu-Guang Ma,[∥] and Hong-Bo Sun*,[†,‡]

State Key Laboratory on Integrated Optoelectronics, College of Electronic Science and Engineering, Jilin University, 2699 Qianjin Street, Changchun 130012, China, College of Physics, Jilin University, 119 Jiefang Road, Changchun 130023, China, Department of Chemistry, Renmin University of China, Beijing 100872, China, and State Key Laboratory on Supramolecular Structures and Materials, College of Chemistry, Jilin University, 2699 Qianjin Street, Changchun 130012, China

Cyano-substituted oligo (α-phenylenevinylene)-1,4-bis(*R*-cyano-4-diphenylaminostyryl)-2,5-diphenylbenzene (CNDPASDB) molecules are studied in solution and aggregate state by time-resolved fluorescence techniques. CNDPASDB exhibits a strong solvent polarity dependent characteristic of aggregation-induced emission (AIE). By time-dependent spectra, the gradual transition from local excited state to intramolecular charge transfer state with the increasing solvent polarity is clearly resolved. The transition time in high polarity solvent DMF is very fast, around 0.5 ps, resulting in a low fluorescence quantum yield. While in aggregate state, the intramolecular torsion is restricted and the local environment becomes less polar. Thus, the intramolecular charge transfer state is eliminated and efficient AIE occurs.

Introduction

Most conjugated molecules show high fluorescence in their dilute solutions but become weakly luminescent in the solid state. However, organic devices such as organic light emitting diodes (OLED) and lasers are only able to function in a film or crystalline state;[1,2] consequently, ideal luminescent material must possess high solid state luminescence. Because Tang and co-workers[3−5] and Park and co-workers[6] have reported several material systems that have aggregation-induced emission (AIE) properties, increasing attention has been paid to enhance the solid-state efficiency of luminescent materials. Different kinds of crystals that show AIE properties have been reported.[7,8] It is suggested that the possible mechanism of the AIE is the inhibition of the nonradiative channel, that is, the vibrational/torsional energy relaxation process that is blocked in the aggregate state. A time-resolved fluorescence study has been conducted to investigate the mechanism of AIE. The Wong group[9] measured PL efficiency and emission lifetime as a function of temperature and viscosity of the solvent, two parameters strongly affecting the torsional and vibrational motion of a molecule, and they concluded that AIE can be ascribed to the deactivation of nonradiative decay caused by restricted torsional motions of the molecules in the solid state. Some other studies have reached a similar conclusion.[10,11] Very recently a new mechanism "restricted twisted intramolecular charge transfer" was suggested by a steady state study on AIE of boron dipyrromethene (BODIPY) derivatives.[12] Actually, the characteristics of intramolecular charge transfer (ICT) with dual fluorescence have been extensively studied in the past 30 years,[13−17] and twisted intermolecular charge transfer (TICT)
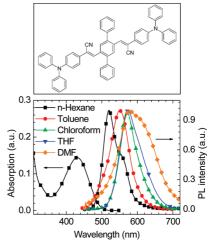

Figure 1. Molecular structure of CNDPASDB (top); Absorption spectrum in hexane (square) and fluorescence spectra in hexane (square), toluene (circle), chloroform (up triangle), tetrahydrofuran (THF, down triangle), and dimethyl formamide (DMF, diamond) at room temperature (bottom).

model,[18−20] planar intramolecular charge transfer (PICT) model,[21,22] and models such as Δ*E*(S1,S2), playing a crucial role in determining the occurrence of ICT state,[23] have been studied. Nevertheless, there are still many controversies on the mechanism of ICT.

Uniaxially oriented molecular crystal cyano-substituted oligo α-phenylenevinylene)-1,4-bis(*R*-cyano-4-diphenylaminostyryl)-2,5-diphenylbenzene (CNDPASDB) (Figure 1) was reported with high luminescence.[24] It also shows a high two-photon absorption cross section (515 GM at 800 nm) and high fluorescence quantum efficiency (30%), which becomes a potential material for organic solid state laser diode and upconversion lasing with low threshold (1.3 mJ pulse⁻¹cm⁻²).[25,26] However, the fundamental properties of the excited state of

* To whom correspondence should be addressed. E-mail: haiyu_wang@jlu.edu.cn (H.-Y.W.); hbsun@jlu.edu.cn (H.-B.S.).
[†] College of Electronic Science and Engineering, Jilin University.
[‡] College of Physics, Jilin University.
[§] Renmin University of China.
[∥] College of Chemistry, Jilin University.

Study of Aggregation-Induced Emission Enhancement

J. Phys. Chem. B, Vol. 114, No. 1, 2010 **129**

CNDPASDB in different solvents and solid states are still not fully understood. CNDPASDB possesses electron donor (diphenylamin) and electron acceptor (cyano) groups in its molecule structure, implying that solvent polarity may have a large affect on the properties of its electronic states.

In this paper, we examined the emission performance of CNDPASDB in different solvents and aggregate states. Indeed, the fluorescence spectra of CNDPASDB show large solvatochromism. In high polar solvents (such as acetone, dimethyl formamide (DMF), and acetonitrile), the molecule exhibits excited state intramolecular charge transfer and quantum yield that is about 150 times lower than that in tetrahydrofuran (THF). Interestingly, AIE properties also significantly change with solvent polarity. The quantum yield of the crystal form (30%) is only about 3 times that in solution THF (9%). However, in DMF/water mixture, the aggregation state gives rise to an almost 300 times increase compared with that in DMF solution. This phenomenon is similar to the recent results of AIE of BODIPY derivatives.[12] These new observations indicate that the previously verified mechanism of the restricted vibrational/torsional relaxation in the aggregation state is not complete in these cases. For non-ICT systems, such as tetraphenylethylene and silole derivatives, the AIE can be explained very well by the restriction of the intramolecular rotation mechanism. However, when donor−acceptor units are introduced into the dye molecule, the ICT process comes into play and AIE is very likely arising from both the restriction of the intromolecular rotation and the restricted low fluorescent or dark state, for example, ICT or TICT state. Actually, the Wong group[9] has also proposed that the enhanced emission in the film or solid state should be a result of arresting the geometry relaxation of the excited fluorescent state to a nonfluorescent state. However, they did not verify the existence of this state experimentally.

To further understand the origin of aggregation-induced emission enhancement, time-resolved fluorescence measurements have been performed at varied wavelengths in different solvents. By reconstructing the time-resolved emission spectra, the gradual transition from local excited (LE) state to ICT state with increasing solvent polarity is clearly resolved. The transition time in DMF is very fast, around 0.5 ps, while in the aggregate state, the intramolecular torsion is restricted and the local environment becomes less polar, thus, the ICT state is eliminated and efficient AIE occurs. We demonstrate that time-resolved emission spectra is a powerful method to investigate AIE process.

Experimental Section

CNDPASDBs were synthesized by a typical Knoevenagel condensation method.[24] Toluene, chloroform, THF, and DMF solutions of CNDPASDB were prepared at the concentration of 2×10^{-5} mol/L. Aggregation state was prepared by slowly injecting concentrated THF solution of CNDPASDB into a THF/water mixture of 90% volume fraction of water when the latter is being stirred. The concentration of the final solution is 2×10^{-5} mol/L. The solutions were clear and stable even after they were kept for more than 1 month. The SEM image shows particles ranging from tens to hundreds of nanometers in size (Figure 2a). Aggregate state in DMF is prepared in the same manner but with 70% water fraction. The SEM image shows that CNDPASDB particles of about 100 nm in size have been formed (Figure 2b).

Absorption spectra were measured by a Shimadzu UV-1700 spectrophotometer at 0.2 nm resolution. Emission spectra were recorded with a Shimadzu RF-5301PC spectrometer at 0.2 nm
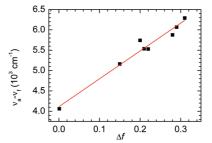

Figure 2. Fluorescence Stokes shifts as a function of orientational polarizability $\Delta f \, (\varepsilon, n)$ in different solvents.

resolution. Nanosecond fluorescence lifetime experiments were performed by the time-correlated single-photon counting (TCSPC) system under right-angle sample geometry. A 379 nm picosecond diode laser (Edinburgh Instruments EPL375, repetition rate 20 MHz) was used to excite the samples. The fluorescence was collected by a photomultiplier tube (Hamamatsu H5783p) connected to a TCSPC board (Becker&Hickel SPC-130). The time constant of the instrument response function (IRF) is about 220 ps.

Subpicosecond time-resolved emission was measured by the femtosecond fluorescence upconversion method. A Nd:YVO laser (Millennia, Spectra Physics) was used to pump a Ti: sapphire laser (Tsunami, Spectra Physics). Its output seeds a regenerative amplifier (RGA, Spitfire, Spectra Physics). The output of the amplifier of 1.5 mJ pulse energy, 100 fs pulse width, at 800 nm wavelength is split into two equal parts; the second harmonic of one beam was focused in the sample as excitation. The resulting fluorescence was collected and focused onto a 1 mm thick BBO crystal with a cutting angle of 35°. The other part of the RGA output was sent into an optical delay line and served as the optical gate for the upconversion of the fluorescence. The generated sum frequency light was then collimated and focused into the entrance slit of a 300 mm monochromator. A UV-sensitive photomultiplier tube 1P28 (Hamamatsu) was used to detect the signal. The electrical signal from the photomultiplier tube was summed by a digital oscilloscope. The relative polarization of the excitation and the gating beams was set to the magic angle. The fwhm of instrument response function was about 500 fs. All the measurements were performed at room temperature.

All the fluorescence transients were fitted to multiexponential functions and were convoluted with the system response function by fixing the long lifetime obtained from TCSPC measurement. The fitting program is ASUFIT (available at www.public.asu.edu/~laserweb/asufit/).

Results and Discussions

Steady State Spectra. Steady state absorbance and emission spectra were measured in different solvents of identical concentration. Solvents are selected with increasing polarity, and the orientational polarizability, Δf, is chosen as the measure of polarity and calculated as follows:[27]

$$\Delta f = \frac{\varepsilon - 1}{2\varepsilon + 1} - \frac{n^2 - 1}{2n^2 + 1} \qquad (1)$$

where ε is the static dielectric constant and n is the optical refractive index of the solvent.

The absorption and emission peaks of CNDPASDB in varied solvents are listed in Tab. 1 including the solvent parameters.

TABLE 1: Steady-State Absorption and Emission Band Peak Positions in Wavelength and Wavenumber Unite and Relative Peak Intensity at Identical Concentrations of CNDPASDB in Different Solvents[a]

solvent	ε	n	Δf	λ_a (nm)	ν_a (cm^{-1})	λ_f (nm)	ν_f (cm^{-1})	ν_a-ν_f (cm^{-1})	I_{PL} (a.u)
n-hexane	1.9	1.375	0.001	430	23255	521	19193	4061	100
benzene	2.27	1.498	0.003	442	22624	555	18018	4606	66
toluene	2.38	1.494	0.014	441	22675	556	17985	4690	50
chloroform	4.81	1.443	0.15	441	22675	571	17513	5163	45
ethyl acetate	6.02	1.37	0.20	430	23255	571	17513	5742	44
tetrahydrofuran	7.58	1.405	0.21	435	22988	573	17452	5536	41
methylene chloride	9.1	1.4244	0.22	438	23831	578	17301	5530	40
dimethyl formamide	36.71	1.428	0.28	432	23148	579	17271	5876	0.28
acetone	20.56	1.356	0.29	429	23310	580	17241	6068	2
acetonitrile	35.94	1.341	0.31	426	23474	582	17182	6292	0.28

[a] The orientational polarizability is calculated as $\Delta f = (\varepsilon - 1)/(2\varepsilon + 1) - (n^2 - 1)/(2n^2 + 1)$.

Normalized emission spectra in typical solvents with increasing polarity are shown in Figure 1b. One can find that CNDPASDB shows the solvatochromism effect: the emission peaks range from 520 nm in *n*-hexane to 580 nm in DMF. In *n*-hexane, it has a clear fine structure, which becomes obscured and red-shifted in toluene and chloroform. In THF, the spectrum is slightly broadened, but the shape does not change much. However, in DMF, it becomes much more broadened, and the spectral shape is much different from those in the other solvents. This solvatochromism can be used to determine the excited state dipole moment μ_E.[28–31] The difference between the ground and the excited state dipole moments can be calculated by the Lippert−Mataga equation:[32,33]

$$\nu_a - \nu_f = \frac{2\Delta f}{hca^3}(\mu_E - \mu_G)^2 + \text{const} \qquad (2)$$

ν_a and ν_f represent the maximum absorbance and fluorescence wavenumbers, respectively, μ_G and μ_E represent the ground state and excited molecular dipole moments, respectively, and a is the Onsager solvent cavity radius. Figure 2 shows the stokes shifts plotted as a function of orientational polarizability, Δf (ε, n). The cavity radius is estimated to be 9 Å, and from the slope, a dipole moment difference of 22 D is obtained. Because the CNDPASDB molecule is symmetric in structure, μ_G is 0 D, so μ_E is 22 D.

At the same concentration, it is noticed that the fluorescence keeps similar intensity in weak or medium polar solvent (from *n*-hexane to THF). However, the relative intensity decreases almost 150 times in high polar solvents, such as DMF, acetone, and acetonitrile. Dramatically changed spectra shape and intensity in DMF solution clearly indicates the formation of a new state (ICT). It maybe also formed in THF but with very small fraction. This assumption is further confirmed in the following time-resolved spectra experiments.

To study the AIE property of CNDPASDB, the steady state fluorescence is recorded in THF, THF/water mixture (Figure 3a), DMF, and DMF/water mixture (Figure 3b) with identical concentration. The SEM image shows that the aggregate state has been formed in the mixture solvents (Figure 3c). The emission intensity is nearly doubled in the aggregate state than that in pure THF, without showing strong enhancement. However, the emission intensity in the DMF/water mixture is almost 300 times stronger than that in pure DMF and its half width at half-maximum (HWHM), after normalization, is even narrower (Figure 3d) than that in pure THF, much more like that in pure chloroform. This strong solvent polarity dependent characteristic indicates that the restriction of nonradiative torsional/vibrational relaxation channel is not a main reason
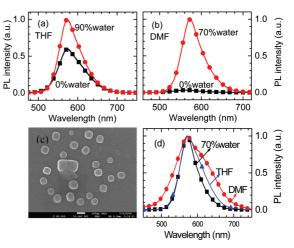

Figure 3. (a) Fluorescence spectra of CNDPASDB in THF/water mixtures with 0 (square) and 90% (circle) water fraction; (b) DMF/water mixture with 0 (square) and 70% (circle) water fraction with identical concentration; (c) SEM photomicrograph of CNDPASDB particles in solution containing 70% volume fraction of water and 30% DMF, the scale down in the figure is 100 nm, with magnification of 8500; (d) normalized steady state fluorescence spectra of CNDPASDB in DMF (circle), THF (up-triangle), and aggregate form (in DMF/water mixture with 70% volume fraction of water; square).

causing AIE, which is essentially not effected by solvent polarity. So we suppose that there must be an additional reason responsible for the low emission in some solvents.

Time-Resolved Fluorescence. To further verify that a new excited state has been formed in DMF, we reconstruct the time-resolved emission spectra (TRES) for all the four solvents and the aggregate states. TRES will show clearly how fluorescence spectra evolute with time and how new states are formed. For each solution, we measured the fluorescence transients at 14−24 different wavelengths. TRES were reconstructed as reported previously.[27] Briefly, all transients are normalized so that their time-integrated values are equal to the intensity of the steady state emission at the corresponding wavelengths. In this way, the normalized fluorescence intensity is known at all times for all detection wavelengths, and thus, the TRES is attained. The time-dependent spectral shifts were characterized by the time-dependent center of gravity in kK ($=10^3$ cm^{-1}), which is proportional to the average energy of emission. The center of gravity in kK is given by[27]

$$\bar{\nu}_{cg}(t) = 10000 \times \frac{\sum_\lambda I(\lambda, t)/\lambda}{\sum_\lambda I(\lambda, t)} \qquad (3)$$

The time-dependent spectral half width, $\Delta\bar{\nu}(t)$ (cm^{-1}), is used to reveal whether the excited state relaxation is described by

Study of Aggregation-Induced Emission Enhancement

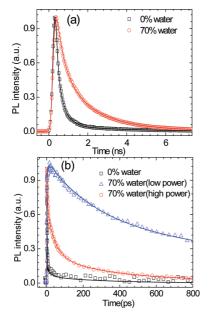*J. Phys. Chem. B, Vol. 114, No. 1, 2010* **131**

Figure 4. Time-resolved peak fluorescence of CNDPASDB in solution with different volume fractions of water and DMF: (a) TCSPC measurement, (b) Up-conversion measurement. The high pump power is 2.5 μJ/pulse, and the low pump power is 500 nJ/pulse. The identical concentration for the mixture is 2×10^{-5}M/L. Emission wavelength: 575 nm.

one or two state models. For data collected at various wavelengths in nanometers, the value of $\Delta\bar{v}(t)$ in kK is given by

$$[\Delta v(t)]^2 = \frac{\sum_\lambda [10000/\lambda - v_{cg}(t)]^2 \times I(\lambda, t)}{\sum_\lambda I(\lambda, t)} \quad (4)$$

A. Comparison of Lifetime between DMF Solution and Aggregate State. For DMF solution (Figure 4), TCSPC gives two long lifetimes: 300 ps and 3.4 ns. Up-conversion measurements reveal two fast components, 1.6 ps (90%) and 27 ps (5%), and the long lifetime of 3.4 ns is hardly seen here. We notice that the emission decays very fast in DMF, and the average lifetime is only about 32 ps. In the aggregate state (Figure 4), the fluorescence decay is excitation power dependent. At high power ($\sim$2.5 μJ/pulse), two short lifetimes have increased to 3.7 ps (33%) and 41 ps (38%), and the percentages reduce. The long lifetimes are 280 ps (21%) and 1.8 ns (4.6%). The average lifetime is 159 ps. When excitation power is low ($\sim$500 nJ/pulse), only two long lifetimes remain, 253 ps (47%) and 1.8 ns (53%), which give much long average lifetime of 1.1 ns. This power-dependent behavior is obviously due to self-quenching (such as exciton−exciton annihilation) in aggregate state when the molecules are much closer to each other.

The significant increased lifetime (more than 30 times) in DMF/water mixture is consistent with the larger increase of quantum yield in aggregate form.

B. Time-Resolved Emission in Toluene and Chloroform. Representative fluorescence transients of CNDPASDB dissolved in toluene, monitored at various detection wavelengths, are given in Figures S1 and S2 in the Supporting Information. The characteristic times are given in Table 2. The intensity decays very quickly on the blue side of the emission and displays a rise on the long wavelength side. The fast decay time constant is 4 ps (50%) at 510 nm, 4.3 ps (23%) at 540 nm, and 12.5 ps (4%) at 560 nm. The time constant is increasing with the

wavelength, and the fraction of the fast component is getting smaller. The rise time constant is 6.5 ps (14%) at 580 nm and 14.3 ps (36%) at 650 nm. We note that for 560 nm, which is very close to the steady state fluorescence peak (556 nm), the fast decay fraction is close to zero. So the turning point from fast decay to the rise is around the peak position. The TCSPC measurements show that the longest lifetime is identical for all wavelengths (2250−2300 ps).

The reconstructed TRES (Figure 5) show that the spectra are decaying slowly, of which the average lifetime for the peak (556 nm) is about 1.92 ns. The time-resolved center of gravity $\bar{v}_{cg}(t)$ (Figure 6a) shows that the spectra have a dynamic stokes shift of 700 cm^{-1} within 20 ps. The spectrum shows an initial narrowing (Figure 6b) with the fwhm decreases for 270 cm^{-1} from 1200 cm^{-1} at $t = 0$ ps to 930 cm^{-1} at $t = 30$ ps. The narrowing is considered mainly caused by the rapid decay (0.4−0.6 ps) in the range from 460 to 500 nm, likely reflecting the vibritional redistribution processes, which typically occurs within hundreds of femtoseconds. The following spectra narrowing within tens of picoseconds comes from the vibrational cooling.[34−36] No emergence of a new state indicates that the excited state dynamics in toluene are dominated by the solvation process.

In chloroform, the fluorescence transients are similar to the dynamics in toluene: the intensity decays quickly on the blue side of the emission and displays a rise on the long wavelength side of the emission (Figure 5 and Table 2). The TCSPC measurements show that the longest lifetimes are almost the same for all wavelengths (2700 ps), indicating the emission is also from one state. However around the fluorescence peak of 571 nm, the transient still shows a large fraction of the fast decay (8 ps, 45%). The turning point is around 600 nm, which is 30 nm red to the emission peak.

Figure 5 shows TRES in chloroform, where the average lifetime for the peak (571 nm) is about 1.32 ns, shorter than that in toluene. The center of gravity $\bar{v}_{cg}(t)$ (Figure 6a) shows that the spectra have a dynamic stokes shift of 300 cm^{-1} within 20 ps; fwhm $\Delta\bar{v}(t)$ (Figure 6b) shows a small initial narrowing, from 650 cm^{-1} at $t = 0$ ps to 620 cm^{-1} at $t = 3$ ps and then a broadening to 650 cm^{-1} at 20 ps. The slight change of the spectra suggests that there is still solely one emitting state. However, the 30 nm red shift of the turning point may imply solvation is not the only process in the excited state. We think that the transition from the LE state to the ICT state may happen in chloroform, but the fraction is very small. With increasing polarity of solvent, this ICT state becomes more and more pronounced, see below.

C. Time-Resolved Emission in THF. In medium polarity solvent, THF (Figures S1 and S2 and Table 2), TCSPC measurement shows that the longest lifetimes are wavelength dependent, around 2.7 ns for wavelengths shorter than 600 nm and about 2 ns for wavelengths longer than 630 nm. The two distinct long lifetimes indicate that there may be two emitting spices with different lifetimes. The 60 nm red shift of the turning point is even larger than that in chloroform.

The reconstructed TRES (Figure 5) show that in the first few picoseconds, a new spectra feature emerges on the red side. Its magnitude is about 10% of the main part. The center of gravity $\bar{v}_{cg}(t)$ (Figure 6a) shows that the spectrum has a dynamic stokes shift of 370 cm^{-1} within 10 ps. In contrast with spectra narrowing in toluene and chloroform, here the spectra shows 50 cm^{-1} broadening during the first 10 ps (Figure 6b). All these indicate a larger portion of transition from LE state to ICT state

TABLE 2: Best-Fit Parameters of Femtosecond Fluorescence Up-Conversion Transients of CNDPASDB in Toluene, Chloroform, THF, and DMF with Function $I \propto \sum_i A_i \exp(- t/\tau_i)^a$

	detection (nm)	τ_1 (ps)	τ_2 (ps)	τ_3 (ps)	τ_4 (ps)	τ_5 (ps)
in toluene	460			0.41 (0.77)	9.7 (0.17)	2252 (0.06)
	510			4 (0.5)	63 (0.12)	2250 (0.38)
	540			4.3 (0.23)	129 (0.16)	2300 (0.61)
	560			12.5 (0.04)	433 (0.15)	2300 (0.81)
	580	6.5 (−0.14)			503 (0.17)	2300 (0.83)
	650	14.3 (−0.36)			118 (0.23)	2300 (0.77)
in chloroform	510			0.47 (0.47)	4.2 (0.47)	2700 (0.06)
	550			4.9 (0.62)	116 (0.1)	2700 (0.28)
	570			8 (0.45)	238 (0.07)	2700 (0.48)
	600	0.4 (−0.2)			363 (0.21)	2700 (0.79)
	630	6.2 (−0.37)			197 (−0.13)	2700 (0.87)
	650	8.9 (−0.5)			426 (0.22)	2700 (0.78)
in THF	510			0.89 (0.71)	6.6 (0.16)	2514 (0.13)
	550			1.9 (0.58)	25 (0.07)	2766 (0.72)
	573			3.6 (0.44)	198 (0.05)	2700 (0.51)
	600			6.2 (0.23)		2300 (0.77)
	630	0.5 (−0.7)				2073 (1)
	670	0.96 (−0.79)	5.9 (−0.21)			2068 (1)
	690	1.2 (−0.83)	15 (−0.17)			2000 (1)
In DMF	490		0.4 (0.97)	12 (0.018)	1500 (0.004)	4000 (0.0002)
	525		0.65 (0.87)	3.4 (0.12)	600 (0.008)	3800 (0.002)
	580		2.1 (0.77)	13 (0.13)	300 (0.094)	3200 (0.006)
	630	0.26 (−1)		4.1 (0.66)	173 (0.32)	2600 (0.01)
	690	0.59 (−1)		6.1 (0.21)	207 (0.78)	2200 (0.01)
	720	0.57 (−1)		3.8 (0.52)	185 (0.47)	2200 (0.01)
aggregate (high power)	515		0.33 (0.62)	2.7 (0.29)	34 (0.085)	1400 (0.005)
	550		2.7 (0.46)	32 (0.35)	213 (0.16)	1400 (0.03)
	570		3 (0.39)	41 (0.37)	283 (0.20)	1800 (0.04)
	635		7 (0.25)	56 (0.41)	409 (0.27)	2200 (0.07)
	690			24 (0.29)	238 (0.51)	2200 (0.20)
aggregate (low power)	575				253 (0.47)	1800 (0.53)

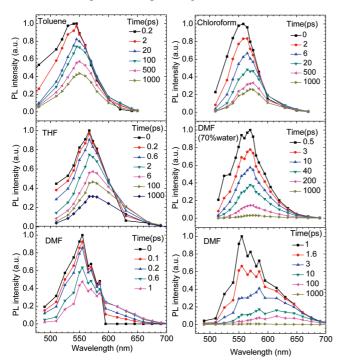^{a} Relative weights (A_i) are given in parentheses.

Figure 5. Reconstructed time-resolved spectra of CNDPASDB in toluene, chloroform, THF, DMF, and DMF/water mixture with 70% volume fraction of water. The uncertainties are within ±5%.

Figure 6. Time-dependent (a) center of gravity, (b) spectra half width in different solvents. The uncertainties are within ±5%.

than in chloroform, as can be observed in TRES. However, the main emitting spices is still the LE state.

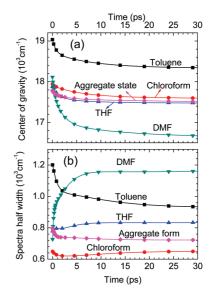**D. Time-Resolved Emission in DMF.** In high polarity solvent, DMF (Figures S1 and S2 and Table 2), the longest lifetimes show very pronounced wavelength-dependent behavior, changing from 4 ns at 490 nm to 2.2 ns at 720 nm. The reconstructed TRES (Figure 5) show that the spectra are decaying very fast. The average lifetime around the peak (580 nm) is about 32 ps, which is much faster than that in the former three solvents (1.3−1.9 ns). During the first 1 ps, accompanying the decay of the main part spectra there is a new spectral feature on the red side. Different from that in THF, here the main part decays to half of the original amplitude in only 1 ps, and a new emerging part grows large enough to be comparable with the

Study of Aggregation-Induced Emission Enhancement

J. Phys. Chem. B, Vol. 114, No. 1, 2010 **133**

main part. It is obvious that the transition from LE state to ICT state is much more efficient in DMF than those in THF and chloroform. The center of gravity $\bar{\nu}_{cg}(t)$ (Figure 6a) shows that the spectrum has initial fast red shift of 1110 cm^{-1}, from 18110 cm^{-1} at 0 ps to 17000 cm^{-1} at 4 ps, then a slow red shift of 360 cm^{-1} to 16640 cm^{-1} at 45 ps, and finally a slow blue shift of 790 cm^{-1} to 17430 cm^{-1} at 1000 ps. The change of the spectral half width is 420 cm^{-1} (Figure 6b), which is much larger than those in chloroform (30 cm^{-1}) and THF (50 cm^{-1}), suggesting that, in DMF, the spectra evolutes by a two state model. The initial LE state has a longer intrinsic lifetime of 4 ns, and the ICT state has a shorter intrinsic lifetime of 2.2 ns. As with decaying, most of the LE state transforms to the ICT state in a few picoseconds, resulting in a red shift and broadening of the spectra, because the ICT state is red to the LE state. Then, the remaining LE state continues to decay together with the ICT state. But because the natural lifetime of LE state is longer than that of the ICT state, the ICT state is decaying faster than the LE state, leading to the slow blue shift of the spectra.

The decay time of the LE state (0.64 ps) matches well with the rise time of the ICT state (0.57 ps), which suggests that the transition time from LE to ICT state is fast, around 0.5−0.6 ps.

E. Time-Resolved Emission of the Aggregate State in DMF/ Water Mixture. Representative fluorescence transients of CND-PASDB aggregate state in DMF/water mixture with a water fraction of 70%, monitored at various detection wavelengths are given in Figures S1 and S2. The characteristic times are given in Table 2. Different from the other four solutions, no rise is found for the red wavelength emission, even at 690 nm, the red-most wavelength of its steady state emission. The longest lifetimes are wavelength-dependent, changing from 1.4 ns at 515 nm to 2.2 ns at 690 nm, which is probably due to heterogeneity of the aggregate state and energy transfer between these states. As we mentioned before, the molecules are so close in the aggregate state that, when irradiated by the focused picosecond (TCSPC) or femtosecond (up conversion) pulses, self-quenching may occur. The fast decay components are the results of the quenching.

The reconstructed TRES (Figure 5) shows no big change of the spectra without any new component emerging. The spectra show a 70 cm^{-1} narrowing within 20 ps (Figure 6b). We tentatively attribute this small narrowing of the spectra half width to the cooling of vibration state just like in toluene. Anyway, the change is much smaller than that in DMF solution (420 cm^{-1}), and the emission can be explained by a single state model, indicating only LE state emitting, without transition to ICT state.

Solvent Polarity Dependent Excited State Dynamics. CNDPASDB solution in various solvents of the same concentration have been excited at the same wavelength (440 nm), and the steady state fluorescence measurements show that the emission intensity becomes smaller with the polarity increasing. Until methylene chloride ($\Delta f = 0.218$), the intensity has decreased only to 40% of that in hexane ($\Delta f = 0.001$). However, from DMF ($\Delta f = 0.275$), the intensity suddenly decreased to 0.28% of that in hexane. We also note that the emission of CNDPASDB red shifts and broadens with the polarity increasing. Especially in solvents of Δf greater than that in DMF, the spectral shape has significantly changed. From these two aspects, we propose that, from DMF on, the ICT state, a relatively dark state, has become the main emitting state, resulting in a sudden decrease in the PL intensity and a great change in the PL spectral

shape. To further study the transition from the LE state to ICT state, time-resolved fluorescence measurements have been conducted.
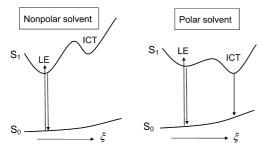
The long time decays are almost the same for all wavelengths in toluene (2.2−2.3 ns) and chloroform (2.7 ns). However, in THF, the long lifetime began to vary with wavelength, ranging from 2.5 ns for 510 nm to 2 ns for 690 ns. In DMF, the change is even obvious, 4 ns for 490 nm and 2.2 ns for 720 nm. The two different long lifetimes indicate there are two emitting spices in THF and DMF.

From the reconstructed TRES we observe that, in toluene and chloroform, the emissions only show spectral decay with time, while in THF and DMF, the decay of the main part is accompanied by a rise of a new feature on the red side, indicating the emergence of an ICT state. However, the rising of the new feature is much efficient in DMF than in THF. The time-dependent center of gravity $\bar{\nu}_{cg}(t)$ indicates that DMF solution shows a much bigger broadening of the spectra (420 cm^{-1}) than those in chloroform (30 cm^{-1}) and in THF (50 cm^{-1}), indicating a much more obvious two-state model in DMF and more likely a single-state model in chloroform and THF. The small broadening of the spectra in chloroform and THF may imply there is a little transition from LE state to ICT state, but the amplitude of the ICT state is so small that it can hardly be detected.

The dynamics at various emission wavelengths show that, for CNDPASDB dissolved in all the four solvents, toluene, chloroform, THF, and DMF, the emission shows a fast decay at short wavelengths and a rise at long wavelengths, which is a characteristic feature of solvent relaxation. However, the turning points from the fast decay to the rise are not all at the steady state emission peak, but are more feasibly shifted to the red for solvents of higher polarity. The turning point is around the emission peak for toluene. In chloroform and THF, the turning points were red-shifted 30 and 60 nm from the peak, respectively. In DMF, even though from 630 nm (50 nm red to the peak), the emission begins to show a rise taking a few hundred femtoseconds. This is different from the other three solvents, where a fast decay still exists and takes a pretty big fraction, so that the dynamics never show a flat or slow rise for the first tens of picoseconds. The red shift of the turning point indicates that, in toluene, the dynamic stokes shift is only caused by solvation process. For chloroform, THF and DMF, besides solvation, excited state reaction, transition from LE state to ICT state, has occurred. The more red shift of the high polarity solution shows the extent of the transition from LE state to ICT state are getting bigger from chloroform to THF, and the still existing fast decay at long wavelength in DMF shows that the transition is much more efficient than the former two.

The TRES of aggregate state in DMF/water mixture shows only decay without any rising of new component. The change of the spectra half width (70 cm^{-1}) is much smaller than that in DMF (420 cm^{-1}). It shows that in aggregate state, there is no transition from LE state to ICT state, and the only emitting state is the LE state.

So far we have experimentally observed another excited dark state, here for CNDPASDB is the ICT state, which accounts for the low quantum yield in solvents of high polarity like DMF. More detailed examination of the dynamics shows that even in the low polarity solvents like chloroform and THF, ICT state also exists, but with an extremely small fraction so that the emission intensity (mainly from LE state) does not decrease much comparing with that in hexane. The fraction of ICT state increases with the increasing polarity. The potential energy

SCHEME 1

Nonpolar solvent | Polar solvent
S₁ LE ICT | S₁ LE ICT
S₀ ξ | S₀ ξ

surfaces describing the LE → ICT reaction are depicted in Scheme 1. The reaction coordinate ξ involves changes in molecular conformation versus bond length and bond angles. In nonpolar solvents, LE is the lowest excited state and the emission comes mainly from the LE state. Because the ICT state usually has a higher dipole moment than the LE state, it is more stabilized by the solvent and the energy level of two states becomes close to each other as the polarity of the solvent gets higher and higher. There is a chance for the ICT state to occur in solvents like chloroform and THF, but with a very small fraction. When the polarity reaches a certain value, like that in DMF, the ICT state becomes even lower than the LE state so that the emission is mainly from the ICT state. The conformation of the ICT state is quite different from the Franck−Condon ground state, so the transition rate is low and the ICT state is a relatively dark state, which explains low emission intensity in DMF.

For CNDPASDB, the crystal form already shows the torsion angles between the double bond and two adjacent phenyl rings are $\theta_1 = 36$ and $\theta_2 = 31°$, respectively.[22] It is possibly because the ICT state is accompanied by a more twisted conformation of diphenylamino group relative to the central benzene, which may be more close to the twisted ICT model.

Conclusions

In this work, time-resolved fluorescence measurements on CNDPASDB have been performed at various wavelengths in different solvents to better understand the origin of aggregation-induced emission enhancement. By reconstructing the time-resolved emission spectra, the gradual transition from the LE state to the ICT state with increasing solvent polarity is clearly resolved. The transition time in DMF is very fast, around 0.5 ps. In the aggregate state, the intramolecular torsion is restricted, and the local environment becomes less polar, thus, the ICT state is eliminated and efficient AIE occurs. We conclude that, for the molecular CNDPASDB, the mechanism for AIE is not only induced by the restriction of the torsional motion of the molecules, but in the mean time, by the restriction of the transition from the LE state to the ICT state that accompanies the twist. It is consistent with the mechanism suggested very recently of a steady state study on AIE of BODIPY derivatives. The understanding is important for exploring high efficiency OLED and laser devices.

Supporting Information Available: Up-conversion fluorescence transients of CNDPASDB at different detection wavelengths. This material is available free of charge via the Internet at http://pubs.acs.org.

References and Notes

(1) Zhang, D. D.; Feng, J. J.; Liu, Y. F.; Zhong, Y. Q.; Bai, Y.; Jin, Y.; Xie, G. H.; Xue, Q.; Zhao, Y.; Liu, S. Y.; Sun, H. B. *Appl. Phys. Lett.* **2009**, *94*, 223306.

(2) Xia, H.; Li, M.; Lu, D.; Zhang, C. B.; Xie, W. J.; Liu, X. D.; Yang, B.; Ma, Y. G. *Adv. Funct. Mater.* **2007**, *17*, 1757.

(3) Luo, J.; Xie, Z.; Lam, J. W. Y.; Cheng, L.; Chen, H.; Qiu, C.; Kwok, H. S.; Zhan, X.; Liu, Y.; Zhu, D.; Tang, B. Z. *Chem. Commun.* **2001**, 1740.

(4) Chen, J.; Law, C. C. W.; Lam, J. W. Y.; Dong, Y.; Lo, S. M. F.; Williams, I. D.; Zhu, D.; Tang, B. Z. *Chem. Mater.* **2003**, *15*, 1535.

(5) Ran, Y.; Lam, J. W. Y.; Dong, Y.; Tang, B. Z.; Wong, K. S. *J. Phys. Chem. B* **2005**, *109*, 1135.

(6) An, B. K.; Kwon, S. K.; Jung, S. D.; Park, S. Y. *J. Am. Chem. Soc.* **2002**, *124*, 14410.

(7) Xie, Z. Q.; Yang, B.; Li, F.; Cheng, G.; Liu, L. L.; Yang, G. D.; Xu, H.; Ye, L.; Hanif, M.; Liu, S. Y.; Ma, D. G.; Ma, Y. G. *J. Am. Chem. Soc.* **2005**, *127*, 14152.

(8) Li, Y. P.; Li, F.; Zhang, H. Y.; Xie, Z. Q.; Xie, W. J.; Xu, H.; Li, B.; Shen, F. Z.; Ye, L.; Hanif, M.; Ma, D. G.; Ma, Y. G. *Chem. Commun.* **2007**, 231.

(9) Ren, Y.; Lam, W. Y.; Dong, Y. Q.; Tang, B. Z.; Wong, K. S. *J. Phys. Chem. B* **2005**, *109*, 1135.

(10) Ren, Y.; Dong, Y. Q.; Lam, J. W. Y.; Tang, B. Z.; Wong, K. S. *Chem. Phys. Lett.* **2005**, *402*, 468.

(11) Lee, M. H.; Dong, Y. Q.; Tang, B. Z.; Kim, D. *J. Korean Phys. Soc.* **2004**, *45*, 329.

(12) Hu, R.; Lager, E.; Aguilar-Aguilar, A.; Liu, J.; Lam, J. W. Y.; Sung, H. H. Y.; Williams, I. D.; Zhong, Y.; Wong, K. S.; Pea-Cabrera, E.; Tang, B. Z. *J. Phys. Chem. C* **2009**, *113*, 15845.

(13) Ma, C.; Kwok, W. M.; Matousek, P.; Parker, A. W.; Phillips, D.; Toner, W. T.; Towrie, M. *J. Phys. Chem. A* **2002**, *106*, 3294.

(14) Zilberg, S.; Haas, Y. *J. Phys. Chem. A* **2002**, *106*, 1.

(15) Dobkowski, J.; Wojcik, J.; Kozmínski, W.; Kołos, R.; Waluk, J.; Michl, J. *J. Am. Chem. Soc.* **2002**, *124*, 2406.

(16) Zachariasse, K. A. *Chem. Phys. Lett.* **2000**, *320*, 8.

(17) Grabowski, Z. R.; Rotkiewicz, K.; Rettig, W. *Chem. Rev.* **2003**, *103*, 3899.

(18) Grabowski, Z. R.; Rotkiewicz, K.; Siemiarczuk, A.; Cowley, D. J.; Baumann, W. *Nouv. J. Chim.* **1979**, *3*, 443.

(19) Rettig, W. *Angew. Chem., Int. Ed. Engl.* **1986**, *25*, 971.

(20) Rettig, W. In *Topics in Current Chemistry, Electron-Transfer I*; Mattay, J., Ed.; Springer: Berlin, 1994; Vol. 169, p 253.

(21) Il'ichev, Yu. V.; Kuhnle, W.; Zachariasse, K. A. *J. Phys. Chem. A* **1998**, *102*, 5670.

(22) Zachariasse, K. A.; Grobys, M.; von der Haar, Th.; Hebecker, A.; Il'ichev, Yu. V.; Morawski, O.; Ruckert, I.; Kuhnle, W. *J. Photochem. Photobiol. A* **1997**, *105*, 373.

(23) Zachariasse, K. A.; Druzhinin, S. I.; Bosch, W.; Machinek, R. *J. Am. Chem. Soc.* **2004**, *126*, 1705.

(24) Li, Y. P.; Shen, F. Z.; Wang, H.; He, F.; Xie, Z. Q.; Zhang, H. Y.; Wang, Z. M.; Liu, L. L.; Li, F.; Hanif, M.; Ye, L.; Ma, Y. G. *Chem. Mater.* **2008**, *20*, 7312.

(25) Fang, H. H.; Chen, Q. D.; Yang, J.; Xia, H.; Ma, Y. G.; Wang, H. Y.; Sun, H. B. *Opt. Lett.* **2009**, accepted for publication.

(26) Chen, Q. D.; Fang, H. H.; Xu, B.; Yang, J; Xia, H.; Chen, F. P.; Tian, W. J.; Sun, H. B. *Appl. Phys. Lett.* **2009**, *94*, 201113.

(27) Lakowicz, J. R. *Principles of Fluorescence Spectroscopy*; 3rd ed.; Springer: Berlin/Heidelberg, 2006.

(28) Horng, M. L.; Gardechi, J. A.; Papazyan, A.; Maroncelli, M. *J. Phys. Chem.* **1995**, *99*, 17311.

(29) Dahl, K.; Biswas, R.; Ito, N.; Maroncelli, M. *J. Phys. Chem. B* **2005**, *109*, 1563.

(30) Ghazy, R.; Azim, S. A.; Shaheen, M.; El-Mekawey, F. *Spectrochim. Acta, Part A* **2004**, *60*, 187.

(31) Kabatc, J.; Osmialowsk, B.; Paczkowski, J. *Spectrochim. Acta, Part A* **2006**, *63*, 524.

(32) Lippert, V. E. *Z. Electrochem.* **1957**, *61*, 962.

(33) Mataga, N.; Kaifu, Y.; Koizumi, M. *Bull. Chem. Soc. Jpn.* **1956**, *29*, 465.

(34) Kang, T. J.; Ohta, K.; Tominaga, K; Yoshihara, K. *Chem. Phys. Lett.* **1998**, *287*, 29.

(35) Kovalenko, S. A.; Schanz, R.; Henning, H.; Ernsting, N. P. *J. Chem. Phys.* **2001**, *115*, 3256.

(36) Wang, H.; Zhang, H.; Abou-Zied, O. K.; Yu, C.; Romesberg, F. E.; Glasbeek, M. *Chem. Phys. Lett.* **2003**, *367*, 599.